Front. Optoelectron. 2021, 14(4): 438–444
https://doi.org/10.1007/s12200-020-0969-3

RESEARCH ARTICLE

Singular PT-symmetry broken point with infinite transmittance and reflectance—a classical analytical demonstration

Yingxin JIANG (✉)

Department of Physics, Jiangsu University, Zhenjiang 212013, China

Abstract To demonstrate the existence of singular parity-time symmetry (PT-symmetry) broken point in optics system, we designed a one-dimensional PT symmetric structure including N unit-cell with loss and gain materials in half. We performed an analytical deduction to obtain the transmittance and reflectance of the structure basing on Maxwell's equations. We found that with the exact structure unit-cell number and the imaginary part of refraction index, the transmittance and reflectance are both close to infinite. Such strict condition is called the singular point in this study. At the singular point position, both the transmission and reflection are direction-independent. Away from the singular point, the transmittance and reflectance become finite. In light of classical wave optics, the single unit and total structure both become the resonance units. The infinite transmittance and reflectance result from the resonance matching of single unit and total structure. In light of quantum theory, the singular point corresponds to the single eigenvalue of electromagnetic scattering matrix. The infinite transmittance and reflectance mean a huge energy transformation from pumping source to light waves. Numerical calculation and software simulation both demonstrate the result.

Keywords parity-time symmetric (PT-symmetric) structure, singular point, transmittance, reflectance

1 Introduction

In designing optical transmission system, the material refraction indexes take the leading position. Diverse distributions of refractive index have led to great progress in optics ranging from the design and fabrication of photonic crystals [1] and photonic crystal fibers [2] to the exploration of nanoplasmonics [3] and metamaterials with negative refraction effect [4]. For most cases, people consider the ideal dielectric with real refractive index. Loss is a trivial problem that is usually solved by the loss correction or compensation gain [5]. Gain is also used to overcome the loss. For long time, loss and gain have taken a back seat in optics design. However, such a situation has been changed since parity-time symmetric (PT-symmetric) structure was used in optics [6,7].

The PT-symmetric structure comes from quantum mechanics. In quantum mechanics, the parity operator $\hat{p}$ leads to $\hat{x}\to-\hat{x}$ and $\hat{p}\to-\hat{p}$, and the operator $\hat{T}$ leads to $\hat{x}\to\hat{x}$, $i\to-i$ and $\hat{p}\to-\hat{p}$, where $\hat{x}$ and $\hat{p}$ represent the position and momentum operators, respectively. For a non-Hermitian Hamiltonian $\hat{H}=\hat{p}^2/2+V(\hat{x})$ associated with a complex potential $V(\hat{x})$, it is parity-time symmetric provided that it commutes with the parity-time operator, i.e., $\hat{H}\hat{p}\hat{T}=\hat{p}\hat{T}\hat{H}$. In this case, $\hat{H}$ and $\hat{p}\hat{T}$ have a common set of eigenfunctions and the non-Hermitian Hamiltonians can actually possess entirely real spectra as the Hermitian Hamiltonians possess. The lack of completeness or the breaking of PT-symmetry is associated with the presence of exceptional points for the discrete spectrum or the spectral singularity for the continuous spectrum [8].

Matter wave phenomena under the framework of non-Hermitian Hamiltonians are often taken as an analogy study in optical systems with balanced gain and loss, because optics can provide a productive test bed where the notions of parity time symmetry can be experimentally explored. In optics, PT-symmetry demands that the complex refractive index obeys the condition $n(r) = n^*(-r)$, in other words the real part of the refractive index should be an even function of position, whereas the imaginary part must be odd. In these optical systems, gain and loss have played the important role in determining optical properties. Many intriguing physical phenomena

Received September 29, 2019; accepted November 18, 2019

E-mail: jiangyx@mail.ujs.edu.cn

with PT-symmetric systems have been predicted and observed, such as loss induced transparency [9], power oscillations and nonreciprocity of light propagation [7], coherent perfect absorber-lasers [10–12], optical switches [13], on-chip optical isolation [14–16]. The one-dimensional sinusoidal [17,18] and layered PT symmetric complex crystals [19,20] with balanced gain/loss modulations may be highlighted since they show one-way enhanced reflection, while remains total transmission (unidirectional invisibility). The unique phenomena occur at the exception point or PT-symmetry breaking threshold. At the special position, the sum of reflectance and transmittance are larger than unit, which means that the extra energy is obtained from pumping light to the gain regions of the structure. Another important PT-symmetry phenomenon is that the spectral singularities in complex scattering potentials are achieved through an electromagnetic waveguide [8]. At the spectral singularities unbelievable infinite reflectance and transmittance occur. Other researchers also pointed out the existence of novel singular points in the broken-symmetry phase [10–12,21,22]. The singular points are associated to the single eigenvector and eigenvalue of electromagnetic scattering matrix (**S** matrix) [21]. Although the concept of spectral singularities has been introduced into optics system, the analyzed method is also based on quantum theory [8]. In this paper, we demonstrate the existence of the singular broken PT-symmetry points through a classical analytical method from Maxwell equations. Thus our study can provide a more direct demonstration about the singular point. Different from the structures including one unit-cell with loss and gain materials in half embedded in the rectangular waveguide [10–12,21,22], the structure in this study is a one-dimensional model including N unit-cell with loss and gain materials in half. We verify that the singular broken PT-symmetry point has infinite reflectance and transmittance. In this paper. we find that the direct physical reason for the singular point is the exact match between the unit resonance and the system resonance. We also find the singular point just corresponds to the single eigenvalue of the electromagnetic **S** matrix. The results are also demonstrated through numerical calculation and software simulation.

2 Model and analytical deduction

Optical PT-symmetry in one-dimensional structure requires the complex refractive index distributed in x direction in the form of $n(x) = n^*(-x)$. In this paper we construct such PT symmetric structure by placing two layers A and B with the same thickness d alternately in the x-axis. The refraction indexes for layers A and B are chosen as $n_{\mathrm{A}} = n_0 + \mathrm{i}\rho$ and $n_{\mathrm{B}} = n_0 - \mathrm{i}\rho$, respectively, to satisfy the PT-symmetry condition. The structure is schematized in Fig. 1.

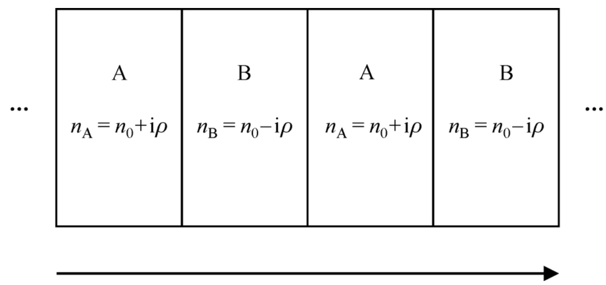

Fig. 1 Schematic diagram of PT symmetric layered structure

For such structure with N period units, we can obtain its transmission properties through strict analytical deduction. For layered structures, the transmittance and reflectance are dependent on the transfer matrixes [23]. The matrixes associated with layers A and B are

$$\boldsymbol{m}_{\mathrm{A}} = \begin{bmatrix} \cos\delta_{\mathrm{A}} & -\mathrm{i}/n_{\mathrm{A}}\sin\delta_{\mathrm{A}} \\ -\mathrm{i}n_{\mathrm{A}}\sin\delta_{\mathrm{A}} & \cos\delta_{\mathrm{A}} \end{bmatrix}, \tag{1}$$

and

$$\boldsymbol{m}_{\mathrm{B}} = \begin{bmatrix} \cos\delta_{\mathrm{B}} & -\mathrm{i}/n_{\mathrm{B}}\sin\delta_{\mathrm{B}} \\ -\mathrm{i}n_{\mathrm{B}}\sin\delta_{\mathrm{B}} & \cos\delta_{\mathrm{B}} \end{bmatrix}, \tag{2}$$

where $\delta_{\mathrm{A}} = n_{\mathrm{A}}k_0 d = n_0 k_0 d + \mathrm{i}\rho k_0 d$ and $\delta_{\mathrm{B}} = n_{\mathrm{B}}k_0 d = n_0 k_0 d - \mathrm{i}\rho k_0 d$ denote the phase change for normal incidence in layers A and B, respectively. For left incidence (from left to right), the matrix for a unit-cell is

$$\boldsymbol{m} = \boldsymbol{m}_{\mathrm{A}}\boldsymbol{m}_{\mathrm{B}} = \begin{bmatrix} m_{11} & m_{12} \\ m_{21} & m_{22} \end{bmatrix} = \begin{bmatrix} \cos\delta_{\mathrm{A}}\cos\delta_{\mathrm{B}} - n_{\mathrm{B}}/n_{\mathrm{A}}\sin\delta_{\mathrm{A}}\sin\delta_{\mathrm{B}} & -\mathrm{i}/n_{\mathrm{B}}\cos\delta_{\mathrm{A}}\sin\delta_{\mathrm{B}} - \mathrm{i}/n_{\mathrm{A}}\sin\delta_{\mathrm{A}}\cos\delta_{\mathrm{B}} \\ -\mathrm{i}n_{\mathrm{B}}\cos\delta_{\mathrm{A}}\sin\delta_{\mathrm{B}} - \mathrm{i}n_{\mathrm{A}}\sin\delta_{\mathrm{A}}\cos\delta_{\mathrm{B}} & \cos\delta_{\mathrm{A}}\cos\delta_{\mathrm{B}} - n_{\mathrm{A}}/n_{\mathrm{B}}\sin\delta_{\mathrm{A}}\sin\delta_{\mathrm{B}} \end{bmatrix}. \tag{3}$$

For the whole periodic structure with N unit-cells, we have the total matrix $\boldsymbol{M}$

$$\boldsymbol{M} = \boldsymbol{m}^N = \begin{bmatrix} M_{11} & M_{12} \\ M_{21} & M_{22} \end{bmatrix} = \begin{bmatrix} m_{11}u_{N-1}(a) - u_{N-2}(a) & m_{12}u_{N-1}(a) \\ m_{21}u_{N-1}(a) & m_{22}u_{N-1}(a) - u_{N-2}(a) \end{bmatrix}, \tag{4}$$

where $a = (m_{11} + m_{22})/2$ and u_N are the Chebyshev Polynomials of the second kind from [23]

$$u_N(a) = \frac{\sin[(N+1)\cos^{-1}(a)]}{\sqrt{1-a^2}}. \tag{5}$$

For background material with refraction index n_0, the transmittance and reflectance of left incidence are respectively

$$T_{\text{left}} = \left| \frac{2n_0}{(M_{11} + M_{22})n_0 + (M_{12}n_0^2 + M_{21})} \right|, \quad (6)$$

$$R_{\text{left}} = \left| \frac{(M_{11} - M_{22})n_0 + (M_{12}n_0^2 - M_{21})}{(M_{11} + M_{22})n_0 + (M_{12}n_0^2 + M_{21})} \right|. \quad (7)$$

To obtain T_{left} and R_{left}, we first calculate the important parameter a. For simplicity, we denote $\delta_A = \delta + i\Delta$ and $\delta_B = \delta - i\Delta$, in which $\delta = n_0 k_0 d$ and $\Delta = \rho k_0 d$. Thus we have

$$\begin{aligned} a &= (m_{11} + m_{22})/2 \\ &= \cos\delta_A \cos\delta_B - \frac{1}{2}\left(\frac{n_B}{n_A} + \frac{n_A}{n_B}\right)\sin\delta_A \sin\delta_B \\ &= \frac{e^{i(\delta+i\Delta)} + e^{-i(\delta+i\Delta)}}{2}\frac{e^{i(\delta-i\Delta)} + e^{-i(\delta-i\Delta)}}{2} \\ &\quad - \frac{1}{2}\frac{n_0^2 - \rho^2}{n_0^2 + \rho^2}\frac{e^{i(\delta+i\Delta)} - e^{-i(\delta+i\Delta)}}{2i}\frac{e^{i(\delta-i\Delta)} - e^{-i(\delta-i\Delta)}}{2i} \\ &= \cos(2\delta + \kappa) = \cos\alpha, \end{aligned} \quad (8)$$

where $\alpha = 2\delta + \kappa$, and κ is a small quantity that is used to correct the approximation of $\frac{n_0^2 - \rho^2}{n_0^2 + \rho^2} = 1$ for $n_0 >> \rho$ used in the conduction of Eq. (8). Here, we make the first constraint condition

$$2\delta = j\pi \ (j = 1, 2, 3...). \quad (9)$$

From $\delta = n_0 k_0 d$, we have

$$d = j\lambda/(4n_0) \ (j = 1, 2, 3...), \quad (10)$$

where λ is the incidence wavelength. Thus we have

$$u_N(a) = \frac{\sin[(N+1)\alpha]}{\sin\alpha}, \quad (11)$$

and

$$M_{11} = m_{11}\frac{\sin(N\alpha)}{\sin\alpha} - \frac{\sin[(N-1)\alpha]}{\sin\alpha}, \quad (12)$$

$$M_{12} = m_{12}\frac{\sin(N\alpha)}{\sin\alpha}, \quad (13)$$

$$M_{21} = m_{21}\frac{\sin(N\alpha)}{\sin\alpha}, \quad (14)$$

$$M_{22} = m_{22}\frac{\sin(N\alpha)}{\sin\alpha} - \frac{\sin[(N-1)\alpha]}{\sin\alpha}. \quad (15)$$

Next basing on $\alpha = 2\delta + \kappa = j\pi + \kappa$, we make following operations.

$$\begin{aligned} M_{11} + M_{22} &= (m_{11} + m_{22})\frac{\sin(N\alpha)}{\sin\alpha} - 2\frac{\sin[(N-1)\alpha]}{\sin\alpha} \\ &= 2\cos\alpha\frac{\sin(N\alpha)}{\sin\alpha} - 2\frac{\sin[(N-1)\alpha]}{\sin\alpha} \\ &= \frac{2}{\sin\alpha}[\cos\alpha\sin(N\alpha) - \sin(N\alpha - \alpha)] \\ &= 2\cos(N\alpha) \\ &= 2\cos(Nj\pi + N\kappa). \end{aligned} \quad (16)$$

For large N, we apply the second constraint condition

$$N\kappa = (N_1 + 1/2)\pi \ (N_1 = 0, \pm 1, \pm 2...). \quad (17)$$

That leads to

$$M_{11} + M_{22} = 0, \quad (18)$$

$$M_{11} - M_{22} = \frac{\pm(m_{11} - m_{22})}{\sin\alpha} = \pm\frac{4i\rho n_0 \sin\delta_A \sin\delta_B}{(n_0^2 + \rho^2)\sin\alpha}, \quad (19)$$

$$M_{12} = \frac{\pm m_{12}}{\sin\alpha}, \quad (20)$$

$$M_{21} = \frac{\pm m_{21}}{\sin\alpha}, \quad (21)$$

$$\begin{aligned} M_{12}n_0^2 &= \frac{\pm m_{12}}{\sin\alpha}n_0^2 \\ &= \pm\left[-i\frac{n_0^2}{n_B}\cos\delta_A\sin\delta_B - i\frac{n_0^2}{n_A}\sin\delta_A\cos\delta_B\right]/\sin\alpha \\ &= \pm[-in_A\cos\delta_A\sin\delta_B - in_B\sin\delta_A\cos\delta_B]\frac{n_0^2}{n_0^2 + \rho^2}/\sin\alpha \\ &= \pm[-in_A\cos\delta_A\sin\delta_B - in_B\sin\delta_A\cos\delta_B]/\sin\alpha. \end{aligned} \quad (22)$$

In Eq. (22), we have made the only approximation in this study for the large contrast of n_0 and ρ

$$\frac{n_0^2}{n_0^2 + \rho^2} \approx 1. \quad (23)$$

Under this approximation, we further have

$$M_{12}n_0^2+M_{21}=\pm[-\mathrm{i}\cos\delta_{\mathrm{A}}\sin\delta_{\mathrm{B}}(n_{\mathrm{A}}+n_{\mathrm{B}})$$
$$-\mathrm{i}\sin\delta_{\mathrm{A}}\cos\delta_{\mathrm{B}}(n_{\mathrm{A}}+n_{\mathrm{B}})]/\sin\alpha$$
$$=\mp\mathrm{i}2n_0(\cos\delta_{\mathrm{A}}\sin\delta_{\mathrm{B}}+\sin\delta_{\mathrm{A}}\cos\delta_{\mathrm{B}})/\sin\alpha, \tag{24}$$

$$M_{12}n_0^2-M_{21}=\pm[-\mathrm{i}\cos\delta_{\mathrm{A}}\sin\delta_{\mathrm{B}}(n_{\mathrm{A}}-n_{\mathrm{B}})$$
$$-\mathrm{i}\cos\delta_{\mathrm{B}}\sin\delta_{\mathrm{A}}(n_{\mathrm{A}}-n_{\mathrm{B}})]/\sin\alpha$$
$$=\pm2\rho(\cos\delta_{\mathrm{A}}\sin\delta_{\mathrm{B}}+\cos\delta_{\mathrm{B}}\sin\delta_{\mathrm{A}})/\sin\alpha, \tag{25}$$

$$\cos\delta_{\mathrm{A}}\sin\delta_{\mathrm{B}}+\cos\delta_{\mathrm{B}}\sin\delta_{\mathrm{A}}$$
$$=\frac{\mathrm{e}^{\mathrm{i}(\delta+\mathrm{i}\Delta)}+\mathrm{e}^{-\mathrm{i}(\delta+\mathrm{i}\Delta)}}{2}\frac{\mathrm{e}^{\mathrm{i}(\delta-\mathrm{i}\Delta)}-\mathrm{e}^{-\mathrm{i}(\delta-\mathrm{i}\Delta)}}{2\mathrm{i}}$$
$$+\frac{\mathrm{e}^{\mathrm{i}(\delta-\mathrm{i}\Delta)}+\mathrm{e}^{-\mathrm{i}(\delta-\mathrm{i}\Delta)}}{2}\frac{\mathrm{e}^{\mathrm{i}(\delta+\mathrm{i}\Delta)}-\mathrm{e}^{-\mathrm{i}(\delta+\mathrm{i}\Delta)}}{2\mathrm{i}}$$
$$=\sin(2\delta). \tag{26}$$

Taking Eqs. (18), (19), (24) and (25) into Eqs. (6) and (7), we obtain

$$T_{\mathrm{left}}=\left|\frac{2n_0}{(M_{11}+M_{22})n_0+(M_{12}n_0^2+M_{21})}\right|$$
$$=\left|\frac{2n_0\sin\alpha}{0\mp2\mathrm{i}n_0\sin(2\delta)}\right|$$
$$=\left|\frac{\sin\alpha}{\sin(2\delta)}\right|, \tag{27}$$

$$R_{\mathrm{left}}=\left|\frac{(M_{11}-M_{22})n_0+(M_{12}n_0^2-M_{21})}{(M_{11}+M_{22})n_0+(M_{12}n_0^2+M_{21})}\right|$$
$$=\left|\frac{\mp\frac{2\rho n_0^2\sin\delta_{\mathrm{A}}\sin\delta_{\mathrm{B}}}{(n_0^2+\rho^2)}\pm\mathrm{i}\rho\sin(2\delta)\sin\alpha}{\pm n_0\sin(2\delta)}\right|. \tag{28}$$

From Eq. (9), we have $\sin(2\delta)=0$. Since $\sin\alpha$, $\sin\delta_{\mathrm{A}}$ and $\sin\delta_{\mathrm{B}}$ are all finite, T_{left} and R_{left} are both close to infinite. The infinite values are based on a special status. Thus Eqs. (9) and (28) state the resonance condition and the resonance amplification effect, respectively. We will demonstrate in the next section that it is a special PT-symmetry broken point. However, we should notice that the infinite T_{left} and R_{left} are based on the constraint conditions of Eqs. (9) and (17). Such conditions lead that such PT-symmetry broken points should be singular and only dependent on the two special structure parameters N and ρ if Eq. (9) holds.

Up to here, one may ask whether the infinite T_{left} and R_{left} occur for only left incidence. In this study, we can demonstrate for right incidence (from right to left) infinite transmittance and reflectance occur at the same parameters N and ρ. In fact, for right incidence the matrix of a unit-cell is

$$\boldsymbol{m}'=\boldsymbol{m}_{\mathrm{B}}\boldsymbol{m}_{\mathrm{A}}=\begin{bmatrix}m'_{11} & m'_{12}\\ m'_{21} & m'_{22}\end{bmatrix}=\begin{bmatrix}\cos\delta_{\mathrm{B}}\cos\delta_{\mathrm{A}}-n_{\mathrm{A}}/n_{\mathrm{B}}\sin\delta_{\mathrm{B}}\sin\delta_{\mathrm{A}} & -\mathrm{i}/n_{\mathrm{A}}\cos\delta_{\mathrm{B}}\sin\delta_{\mathrm{A}}-\mathrm{i}/n_{\mathrm{B}}\cos\delta_{\mathrm{A}}\sin\delta_{\mathrm{B}}\\ -\mathrm{i}n_{\mathrm{B}}\cos\delta_{\mathrm{A}}\sin\delta_{\mathrm{B}}-\mathrm{i}n_{\mathrm{A}}\cos\delta_{\mathrm{B}}\sin\delta_{\mathrm{A}} & \cos\delta_{\mathrm{B}}\cos\delta_{\mathrm{A}}-n_{\mathrm{B}}/n_{\mathrm{A}}\sin\delta_{\mathrm{B}}\sin\delta_{\mathrm{A}}\end{bmatrix}. \tag{29}$$

The total matrix $\boldsymbol{M}'$ is

$$\boldsymbol{M}'=\boldsymbol{m}'^{N}=\begin{bmatrix}M'_{11} & M'_{12}\\ M'_{21} & M'_{22}\end{bmatrix}=\begin{bmatrix}m'_{11}u_{N-1}(a')-u_{N-2}(a') & m'_{12}u_{N-1}(a')\\ m'_{21}u_{N-1}(a') & m'_{22}u_{N-1}(a')-u_{N-2}(a')\end{bmatrix}. \tag{30}$$

From Eq. (30), we easily find that $a'=(m'_{11}+m'_{22})/2=(m_{11}+m_{22})/2=a$. In this condition, we can demonstrate $M'_{11}+M'_{22}=M_{11}+M_{22}$, $M'_{11}-M'_{22}=-(M_{11}-M_{22})$, $M'_{12}=M_{12}$ and $M'_{21}=M_{21}$. Comparing Eqs. (6) and (7) with

$$T_{\mathrm{left}}=\left|\frac{2n_0}{(M'_{11}+M'_{22})n_0+\left(M'_{12}n_0^2+M'_{21}\right)}\right|, \tag{31}$$

$$R_{\mathrm{left}}=\left|\frac{(M'_{11}-M'_{22})n_0+\left(M'_{12}n_0^2-M'_{21}\right)}{(M'_{11}+M'_{22})n_0+\left(M'_{12}n_0^2+M'_{21}\right)}\right|, \tag{32}$$

we find T_{right} is always equal to T_{left}, thus the transmission is always reciprocal. However, without the constraint condition of Eq. (9), $M'_{12}n_0^2-M'_{21}$ is not equal to zero. Because of $M'_{11}-M'_{22}=-(M_{11}-M_{22})$, R_{right} is not equal to R_{left}. Therefore, only at the isolated PT-symmetry broken point with $M'_{12}n_0^2-M'_{21}=0$, the reflection is reciprocal.

3 Demonstration by numerical calculations and simulation

Here we consider a specific example. Taking arbitrary values of $\lambda = 150$ nm and $n_0 = 3$, the value of d is taken as $d = 5\lambda/(4n_0) = 62.5$ nm according to Eq. (10). Thus $T_{\rm left}$ and $R_{\rm left}$ are only dependent on the two parameters N and ρ. Based on Eqs. (6) and (7) and a Matlab program, the 3D plots of $T_{\rm left}(N,\rho)$ and $R_{\rm left}(N, \rho)$ are plotted in Fig. 2. We can see from the figure that there is an isolated point at $N = 149$ and $\rho = 0.0158$ at which both $T_{\rm left}$ and $R_{\rm left}$ are close to infinite. Such result just demonstrates the above analytical formulations. It also demonstrates the existence of the singular PT-symmetry broken point aforementioned. About the point, two features should be mentioned. First, it is achieved through a finite period number and small modulation depth of index. Second, according to the analytical formulations in above section, if $d = 5\lambda/(4n_0)$ holds, the wavelength λ can be arbitrary changed and the PT-symmetry broken point keep its position invariant. For example, if we take $\lambda = 15$ nm and $d = 6.25$ nm, the PT-symmetry broken point still occurs at $N = 149$ and $\rho = 0.0158$. Such feature provides us much flexibility in designing PT-symmetry dependent device. For simplicity, we do not show the result.

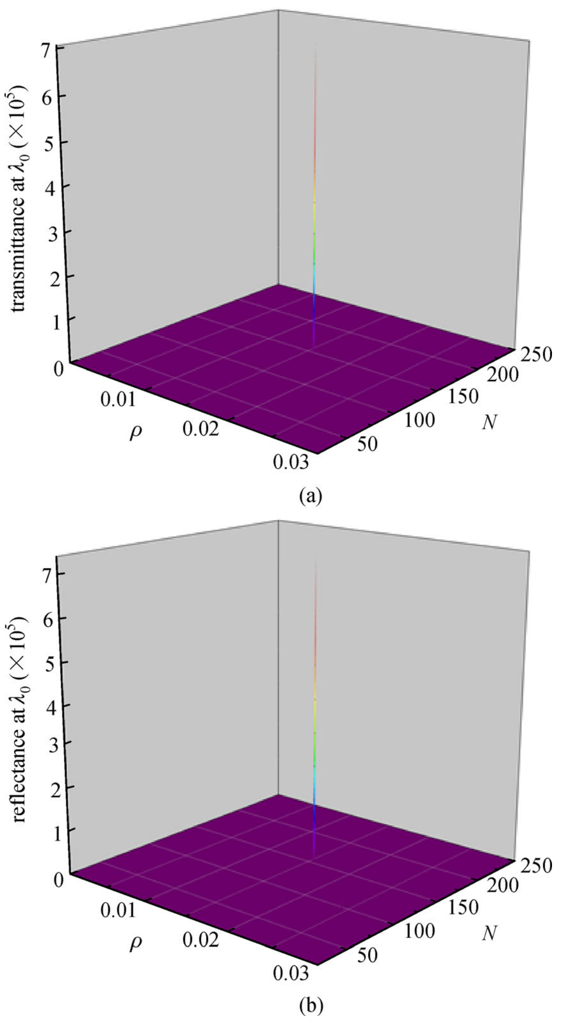

Fig. 2 (a) Transmittance and (b) reflectance for left incidence as a function of N and ρ

The PT-symmetry breaking can be seen from the eigenvalues of scattering matrix $\boldsymbol{S}$ [21,22] that can be deduced from the matrix $\boldsymbol{M}$ in Eq. (4). For PT-symmetric systems, the eigenvalues of the $\boldsymbol{S}$ matrix either form pairs that are unimodular in the exact PT phase, or are with reciprocal moduli in the broken symmetry phase [22]. In Fig. 3, we plot them with different N for $\rho = 0.0158$. It is seen from the figure that out of the range of $145 < N < 153$, all the two eigenvalues are unimodular. The PT-symmetry broken occurs in the range $145 < N < 153$ in which the two eigenvalues form reciprocal relation. However, in the range $145 < N < 153$, the two eigenvalues take a jumping just at $N = 149$ at which they are close to infinite and zero, respectively. The singularity of eigenvalues just corresponds to the singular PT-symmetry broken point. The dependence of the singular PT-symmetry broken point on N means that the structure length plays an important role in determining the optical properties of layered PT-symmetric structure. Some similar results have been reported [18,19]. In Ref. [18], authors proposed sinusoidal PT-symmetric complex crystals of finite thickness and found three regimes of lengths in which the structure takes on different properties. In Ref. [19], authors proposed periodic multilayer structures with PT that exhibits anisotropic reflection oscillation patterns as the number of unit-cells is increasing. Different from those in Refs. [18,19], the reflection and transmission in our study are close to infinite and occur at the isolated PT-symmetry broken point.

To explore the transmission mechanism of infinite $T_{\rm left}$ and $R_{\rm left}$, we perform a simulation through Comsol software based on finite element method. We use a 2D

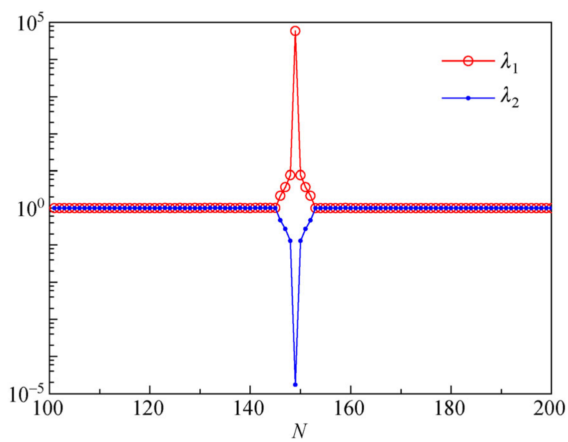

Fig. 3 Two eigenvalues of the $\boldsymbol{S}$ matrix with $\rho = 0.0158$ as a function of N

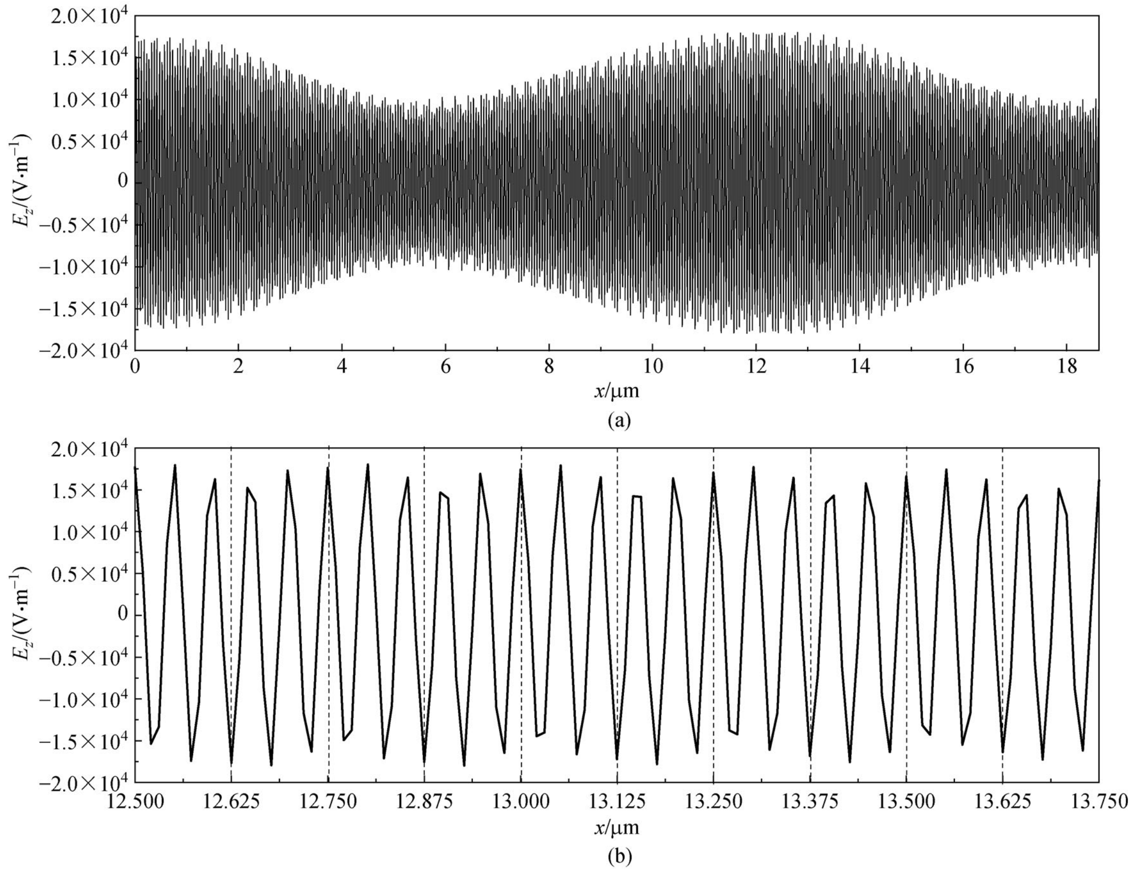

Fig. 4 (a) E_z field distribution inside the PT-symmetric structure at the singular PT-symmetry broken point; (b) localized amplification of (a)

structure in the xy plane instead of infinite one-dimensional structure in x direction and periodic boundary condition in the y direction. We also use two ports at the two interfaces of the 2D structure to excite plane wave with E_z field. The source field value is taken as 0.02 V/m. We perform a frequency domain simulation with incidence wavelength λ = 150 nm and the structure parameters as given in Section 2. The results are shown in Fig. 4(a), through which we find huge field amplification in the PT-symmetric structure. Figure 4(b) is the localized region of Fig. 4(a). The dashed lines denote the interfaces of each unit cell. We clearly find that every interface is exactly at the localized maximum value or minimum value, which means an intense resonance effect occurring at the interfaces. Physically, besides each unit-cell can be function as a resonance unit, the whole structure forms a resonance system. Only if the unit resonance and the system resonance are exactly matched, can the infinite transmittance and reflectance occur. The matched condition is dependent on the values of N and ρ. Because this is an open system, the coupled resonance leads to a huge energy transformation from pumping energy source into the gain regions of the structure. The energy transformation will bring about the infinite transmittance and reflectance.

4 Conclusion

In this paper, we constructed a simple one-dimensional PT-symmetric structure in which the unit cell includes two layers with the conjugated refraction indexes. We found a singular PT-symmetry point corresponding to a special unit cell number and parameter ρ. At the singular PT-symmetry point, infinite transmittance and reflectance simultaneously occur. At the singular point position, both the transmission and reflection are direction-independent. Away from the singular point, the transmittance and reflectance will become finite. Such result means a huge energy transformation from pumping source to light waves. This study demonstrates the quantum theory for the singular point of PT-symmetry system is well in agreement with the classical analysis from the wave optics. Undoubtedly, the strange optical phenomena can be applied in nonlinear optics, energy transformation or other functional optical devices.

References

1. Joannopoulos J D, Villeneuve P R, Fan S. Photonic crystals: putting new twist on light. Nature, 1997, 386(6621): 143–149

2. Knight J C, Broeng J, Birks T A, Russell P S J. Photonic band gap guidance in optical fibers. Science, 1998, 282(5393): 1476–1478
3. Barnes W L, Dereux A, Ebbesen T W. Surface plasmon subwavelength optics. Nature, 2003, 424(6950): 824–830
4. Shelby R A, Smith D R, Schultz S. Experimental verification of a negative index of refraction. Science, 2001, 292(5514): 77–79
5. Marani R, D'Orazio A, Petruzzelli V, Rodrigo S G, Martin-Moreno L, Garcia-Vidal F J, Bravo-Abad J. Gain-assisted extraordinary optical transmission through periodic arrays of subwavelength apertures. New Journal of Physics, 2012, 14(1): 013020
6. Feng L, Xu Y L, Fegadolli W S, Lu M H, Oliveira J E, Almeida V R, Chen Y F, Scherer A. Experimental demonstration of a unidirectional reflectionless parity-time metamaterial at optical frequencies. Nature Materials, 2013, 12(2): 108–113
7. Rüter C E, Makris K G, El-Ganainy R, Christodoulides D N, Segev M, Kip D. Observation of parity–time symmetry in optics. Nature Physics, 2010, 6(3): 192–195
8. Mostafazadeh A. Spectral singularities of complex scattering potentials and infinite reflection and transmission coefficients at real energies. Physical Review Letters, 2009, 102(22): 220402
9. Guo A, Salamo G J, Duchesne D, Morandotti R, Volatier-Ravat M, Aimez V, Siviloglou G A, Christodoulides D N. Observation of PT-symmetry breaking in complex optical potentials. Physical Review Letters, 2009, 103(9): 093902
10. Longhi S. PT-symmetric laser absorber. Physical Review A, 2010, 82(3): 031801
11. Chong Y D, Ge L, Stone A D. PT-symmetry breaking and laser-absorber modes in optical scattering systems. Physical Review Letters, 2011, 106(9): 093902
12. Ge L, Chong Y D, Rotter S, Tureci H E, Stone A D. Unconventional modes in lasers with spatially varying gain and loss. Physical Review A, 2011, 84(2): 023820
13. Nazari F, Nazari M, Moravvej-Farshi M K. A 2×2 spatial optical switch based on PT-symmetry. Optics Letters, 2011, 36(22): 4368–4370
14. Bender N, Factor S, Bodyfelt J D, Ramezani H, Christodoulides D N, Ellis F M, Kottos T. Observation of asymmetric transport in structures with active nonlinearities. Physical Review Letters, 2013, 110(23): 234101
15. Nazari F, Bender N, Ramezani H, Moravvej-Farshi M K, Christodoulides D N, Kottos T. Optical isolation via PT-symmetric nonlinear Fano resonances. Optics Express, 2014, 22(8): 9574–9584
16. Peng B, Özdemir S K, Lei F, Monifi F, Gianfreda M, Long G L, Fan S H, Nori F, Bender C M, Yang L. Parity-time-symmetric whispering-gallery microcavities. Nature Physics, 2014, 10(5): 394–398
17. Lin Z, Ramezani H, Eichelkraut T, Kottos T, Cao H, Christodoulides D N. Unidirectional invisibility induced by PT-symmetric periodic structures. Physical Review Letters, 2011, 106(21): 213901
18. Longhi S. Invisibility in PT-symmetric complex crystals. Journal of Physics A, Mathematical and Theoretical, 2011, 44(48): 485302
19. Zhu X F, Peng Y G, Zhao D G. Anisotropic reflection oscillation in periodic multilayer structures of parity-time symmetry. Optics Express, 2014, 22(15): 18401–18411
20. Ding S, Wang G P. Extraordinary reflection and transmission with direction dependent wavelength selectivity based on parity-time-symmetric multilayers. Journal of Applied Physics, 2015, 117(2): 023104
21. Born M, Wolf E. Principles of Optics: Electromagnetic Theory of Propagation, Interference and Diffraction of Light. Elsevier, Cambridge University, 1997
22. Ge L, Chong Y D, Stone A D. Conservation relations and anisotropic transmission resonances in one-dimensional PT-symmetric photonic heterostructures. Physical Review A, 2012, 85(2): 023802
23. Schomerus H. Quantum noise and self-sustained radiation of PT-symmetric systems. Physical Review Letters, 2010, 104(23): 233601

Yingxin Jiang obtained her master's degree from Lanzhou University, Lanzhou (China), in 2006. In 1999, as a teacher she joined the Department of Physics, Jiangsu University, Zhenjiang, China. In 2012, she was elected as an associate professor. Her research interests include optical physics.